

Pressure-Induced Two-Color Photoluminescence and Phase Transition of Two-Dimensional Layered MnCl_2

Zhipeng Yan, Nana Li, Linyan Wang, Zhenhai Yu, Mingtao Li, Jinbo Zhang, Xiaodong Li, Ke Yang, Guoying Gao,* and Lin Wang*



Cite This: *J. Phys. Chem. C* 2020, 124, 23317–23323



Read Online

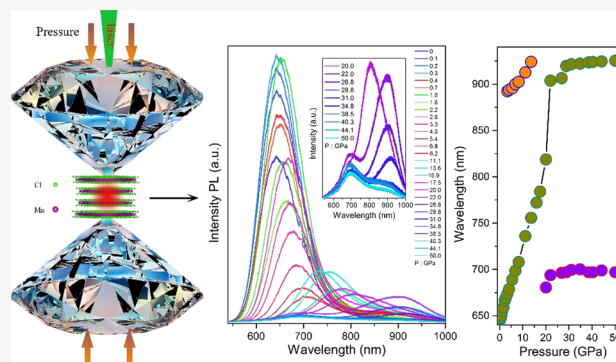
ACCESS |

Metrics & More

Article Recommendations

Supporting Information

ABSTRACT: The transition metal ions are often used to enhance the photoluminescent efficiency in many compounds, which are always received as scintillators, optical sensors and memories, laser media, optoelectronic devices, etc. The photoluminescence of two-dimensional layered transition metal materials, which is associated with electron excitation, has long been the focus of applied materials studies. Most photoluminescence of materials was reported to exhibit redshift and quenched emission as pressure increases. Here, we report the pressure effect on photoluminescence and the correlations with structural phase transitions of manganese dichloride (MnCl_2). A remarkable emission fluctuation at low pressure (below 12 GPa) is observed, which is ascribed to the competition between the shrinkage and tensile strain of the lattice along the c axis. *In situ* synchrotron X-ray diffraction indicates that the MnCl_2 underwent three structural phase transitions at 4, 21.7, and 47.2 GPa, respectively, which led to the two-color photoluminescence during compression. The structural transitions are further confirmed by theoretical calculations. Raman scattering experiments are consistent with XRD, supporting the occurrence of structural transitions. This study provides a comprehensive characterization of the correlation between structural and photoluminescence properties of MnCl_2 at high pressure. The analysis of optical and X-ray diffraction data suggests the important clues for improving photoluminescence performance and an expansive research prospects for two-dimensional layered transition metal halide materials, toward realizing novel material designs.



1. INTRODUCTION

The layered transition metal dihalide (TMD) materials are characterized by extended crystalline planar structures held together by strong intralayer covalent and/or ionic bonds and weak interlayer van der Waals force.¹ The interesting phenomenon observed in the family of TMDs is the wide optical band gap and large resistivity, which makes them ideal optical materials for applications.^{2–5} The traditional manganese dichloride (MnCl_2) is important both in practical applications and in fundamental science, which has attracted significant research interest in decades. Mn possesses the $3d^54s^2$ electronic configuration, and the manganese ion with various valences presents very abundant photoelectric properties, which is paid significant attentions to the band gap and photoluminescence (PL) of manganous compounds (MCs).⁶ As the development and improvement of characterization technology, further exploration of the physical properties of MCs in this work is motivated by their potential in optical applications.^{7,8}

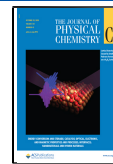
Recent investigations in MnCl_2 indicated that it can be treated as an ideal catalyst and doping material.^{9–11} It was found that MnCl_2 could effectively improve the catalytic

activity for an organic conversion rate.¹² Zihlif *et al.* found that the optical energy gap of poly(ethylene oxide) decreased with the increase of the doping concentration of MnCl_2 .¹³ It was concluded that MnCl_2 filled into PVDF (polyvinylidene fluoride) films exhibit minimum widths of two optical gaps.¹⁴ Ronda *et al.* reported that the absorption and emission of manganese dichloride exhibited a broad band, which interpreted the ${}^4\text{T}_{1g}(\text{G}) \rightarrow {}^6\text{A}_{1g}(\text{S})$ crystal field transition of the Mn^{2+} ion. It was also confirmed that the emission intensity and the decay time of the luminescence of MnCl_2 decrease with the increasing temperature.¹⁵ Sugiura discussed about the mechanism on the shift of the absorption peak to low energy for different transition metal dihalides, which was ascribed to the $4p$ state of the transition metal ion.^{16,17} Most of research efforts aimed to improve PL in those materials, but the

Received: July 19, 2020

Revised: September 28, 2020

Published: September 29, 2020



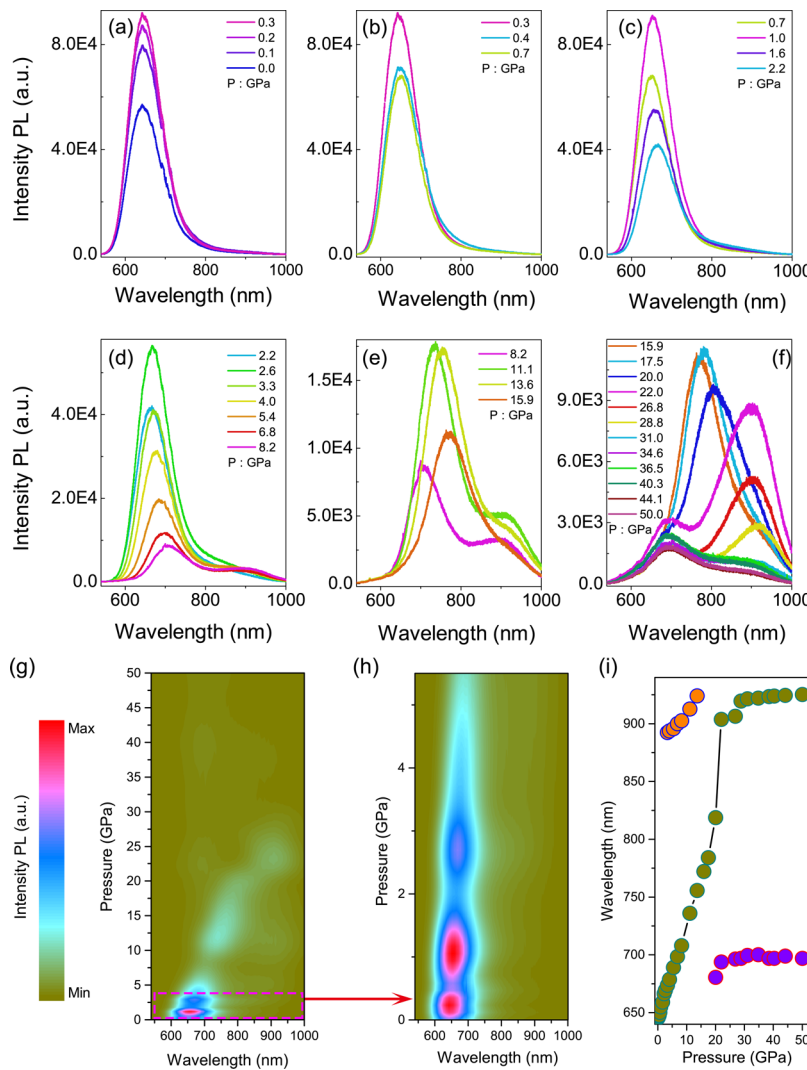


Figure 1. Pressure-induced novel PL spectra of MnCl_2 under various pressures. (a)–(f) Variation of the MnCl_2 emission spectrum with an increase in pressure illustrates PL trapping in the de-excitation processes. (g), (h) Color map of normalized PL intensity of MnCl_2 with a function of pressure. (i) Redshift of PL at various pressures.

microscopic process governing the excited state and de-excitation yielding PL are still not understood fully.¹⁸ Only a few studies of this luminescence in pure MnCl_2 and a significant head-to-head content were implied, where the multivalent manganese was associated by the optical emission spectrum. It is well known that compression can significantly alter the properties of matter, changing the atomic distance and stacking symmetry.^{19,20} For instance, the emission enhancement in halide perovskite due to the increase in exciton binding energy by high pressure.²¹ Thus, a high-pressure technique is applied to explore the mechanism of luminescence for MnCl_2 in this study.

In this letter, we investigate the optical properties and phase transformation of MnCl_2 at high pressure by using the combination of PL, Raman, XRD, and UV-vis absorption with a diamond anvil cell (DAC). Structural evolution is accurately tracked and analyzed by *in situ* XRD and Raman scattering spectra. It was found that pressure-induced two-color photoluminescence and three structural phase transitions occurred in MnCl_2 . The high-pressure phases fulfill the reduction of the nonradiative center and the formation of new luminescence centers for different sites of Mn^{2+} in the

lattice. The ground state electrons benefit from the narrowing band gap in the compression process.²² Our results provide a view for us to further understand the mechanism of structural photoluminescence at high pressure, which will improve the development of layered transition metal halide materials in the field of photoluminescence.

2. EXPERIMENTAL PROCEDURES

Commercial MnCl_2 powder (ultradry, 99.99%) was purchased from Alfa Aesar. The symmetric DAC was used to generate high pressure on the sample. Rhodium gaskets were used in the experiments. The shift of the ruby fluorescence peak was employed for pressure calibration,²³ and silicone oil was used as a pressure transmitting medium. High-pressure ultraviolet–visible absorption measurements were performed on a UV–vis absorption and transmission spectrometer system (UV–vis ATSS) in a DAC with two type II diamonds up to 67.4 GPa. The high-pressure XRD experiments of MnCl_2 were investigated at the Beijing Synchrotron Radiation Facility (BSRF, 4 W2 beamline) and Shanghai Synchrotron Radiation Facility (SSRF, 15 U1 beamline). Both series of experiments were performed with $\lambda = 0.6199 \text{ \AA}$ and the 2D image data were

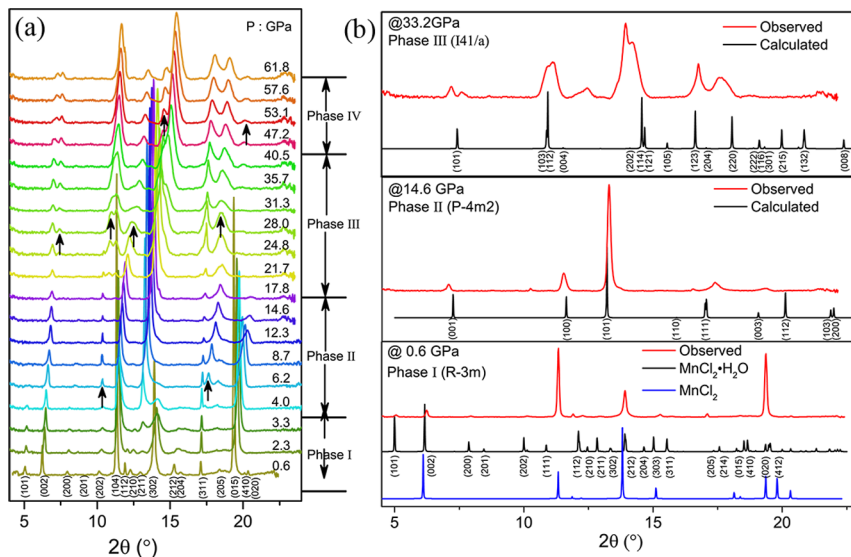


Figure 2. (a) Room temperature synchrotron ($\lambda = 0.6199 \text{ \AA}$) XRD patterns for MnCl_2 under compression up to 61.8 GPa. (b) Calculated XRD patterns with three space groups at different pressures.

integrated using Dioptas software.²⁴ Raman scattering and photoluminescence measurements used an Nd-YAG 532 nm laser and an optical grating of 1200 1/mm,^{25,26} and spectral resolution was less than 1 cm^{-1} .

3. RESULTS

3.1. Photoluminescence Spectrum. The PL properties of MnCl_2 at high pressure are investigated up to 50 GPa, as shown in Figure 1. At ambient conditions, the PL of MnCl_2 at 642 nm (1.93 eV) corresponds to the ${}^4\text{T}_1 \rightarrow {}^6\text{A}_1$ transition within the D_{3d} symmetry (MnF_6)⁴⁻ unit of the CdCl_2 -type structure.²⁷ It can be interpreted that MnCl_2 in the weaker crystal field was associated with Mn^{2+} reflecting its local symmetry. As shown in Figure 1(a)–(d), the fluctuation of PL intensity and emission redshifts is observed in MnCl_2 with the increasing pressure due to the population of deeper Mn^{2+} centers. At 4 GPa (Figure 1(d)), the emergence of the new PL peak is observed at 905 nm, which is associated with two different Mn^{2+} centers: a regular Mn^{2+} site and a perturbed Mn^{2+} site, respectively. Above 22 GPa, another new peak is observed at 693.9 nm as displayed in Figure 1(f). Two possibilities were responsible for the emergence of the new peaks of PL in the MnCl_2 crystal at high pressure: phase transition and chemical reaction. Except for the pressure transmitting medium, there is only MnCl_2 in the chamber and excludes the possibility of a chemical reaction. The pressure-induced change of the symmetry of MnCl_2 makes the difference in energy transfer of the excited state in different Mn^{2+} centers. Thus, we speculate that pressure-induced two-color PL in MnCl_2 is due to the structural phase transition. All of emission spectra indicate that red PL mainly occurs through ligand field changes for the high pressure phase. The PL is robust and could be preserved up to 50 GPa. The color map of the PL intensity of MnCl_2 as a function of pressure is shown in Figure 1(g), and the details of the PL intensity changes below 5 GPa is shown in Figure 1(h), which show the intensity fluctuation clearly. The PL intensity of MnCl_2 is enhanced by pressure, originating from the increase in the exciton binding energy upon lattice shrinkage. Previous works also demonstrated a similar phenomenon in which the exciton binding

energy is increased linearly under high pressure due to the squeezing of the lattice of semiconductor quantum materials.^{21,28–30} The peak positions of PL of MnCl_2 dependent on pressure is plot in Figure 1(i). Both emission bands correspond to the different Mn^{2+} coordinations in the crystal structure.

3.2. X-ray Diffraction at Various Pressures. To elucidate the unusual changes of the PL at high pressure, *in situ* high pressure synchrotron XRD experiments were carried out. The selected XRD patterns up to 61.8 GPa are shown in Figure 2(a). At ambient pressure, MnCl_2 crystallizes in the layered CdCl_2 -type structure (space group, $R\bar{3}m$),³¹ which contains triangular nets of Mn in edge sharing octahedral coordination forming layers of the composition MX_2 separated by van der Waals gaps between the Cl anions. At 0.6 GPa, the XRD pattern reveals that MnCl_2 is mixed with a little portion of $\text{MnCl}_2 \cdot \text{H}_2\text{O}$, which is probably due to hydration of MnCl_2 during sample loading. The oxygen atom in water replaces the original chlorine atom while forming a chemical bond with the manganese atom. As the pressure increases, $\text{MnCl}_2 \cdot \text{H}_2\text{O}$ disappears and the structure becomes a pure phase at 3.3 GPa. During compression, the sudden enhancement intensity of the peak at 17.6° and a new peak at 18.2° are observed at 4 GPa, which indicates the compressed *c* axis originating from the vulnerable interaction of the interlayer in MnCl_2 . Thus, the initial phase undergoes the first structural phase transition at the pressure.

The phase transition is completed at 14.6 GPa. We employed CALYPSO^{32–34} to search the new phase using a simulation cell containing up to 4 formula units in the pressure range of 10–50 GPa. As shown in Figure 2(b) and Figure S1, our simulations discovered a tetragonal phase (space group: $P\bar{4}m2$), which is consistent with the experimental results. As compression continues, all Bragg diffraction peaks shifted to a larger 2θ range, and meanwhile, the new peaks are observed at 10.8° and 11.3° at 21.7 GPa. The emergence of these new peaks means that the crystal structure is rearranged again. When pressure is up to 33.2 GPa, the new phase became dominant. The third structure is determined to be a tetragonal ($I4_1/a$) structure. As the pressure increases up to 47.5 GPa, a new peak at around 14.6° start to appear and become stronger

as pressure increases, suggesting that another phase transition occurred in the sample. However, it is quite different between the calculated XRD and the experimental one of the fourth phase, as shown in Figure S1. It is believed there are at least two reasons for the difference. The first is that the structure of MnCl₂ is a two-dimensional structure with a strong anisotropic nature, which causes a strong preferred orientation especially under high pressure. Second, the element manganese is a typical transition metal with strongly correlated electrons, which might reduce the accuracy of simulations. The possible structures for the high-pressure phases are shown in Figure 2(b).

As found from the structural study, the 2D layered transition metal dihalides exhibit obvious anisotropy; the stability of the crystal field is vulnerable at high pressure. With the increase of the pressure, the defects and nonradiation traps could be gradually activated, which will lead to the change of the ion centers and the efficiency of PL. The responsibility for the changes of Mn²⁺ centers is assigned to the structural phase transition, and the intensity fluctuation of PL is attributed to the results of the competition among these effects at high pressure.

3.3. Raman Scattering Spectrum. Raman scattering spectroscopy is a sensitive method for detecting changes of a crystal, which can give microscopic information to understand the novel PL. Two Raman active modes of MnCl₂ as assigned to the in-plane E_{1g}¹ and the out-of-plane A_{1g}¹ were reported.²⁶ The E_{1g}¹ mode is from the vibrations of both Mn and Cl atoms in the basal plane. Also, the A_{1g}¹ mode reflects the vibration of Cl atoms along the *c* axis. We present *in situ* high-pressure Raman spectra of MnCl₂ in Figure 3(a),(b), which shows the

upon compression, and the modes fully reverted to the original structure. The Raman modes activity of Mn²⁺ in different lattice sites is suppressed above 45.7 GPa. Therefore, a sequence of phase transitions can occur by pressure, resulting in the change of PL.

3.4. UV-Vis Absorption Spectrum. To further understand the behavior of ground state electrons, the ultraviolet-visible absorption spectroscopy (UV-vis AS) is shown in Figure 4(a). Figure 4(a) shows the UV-vis absorption spectrum of MnCl₂ at an ambient condition. A sharp absorption edge is detected at about 5.86 eV, showing a large band gap. As the band gap energy is out of the capability of our instrument, the high-pressure UV-vis absorption spectra were taken from 16.7 GPa. With increasing pressure, the absorption edge is suppressed to a lower energy region (redshifts of the absorption edge), indicating the narrowing of the optical band gap (Figure 4(b)). The absorption edges become more and more broadened above 37.5 GPa. The direct band gap (E_g) of MnCl₂ is fitted by the linearized Tauc coordinates ($\alpha \cdot h\nu$)² - $h\nu$ in Figure 4(c). The obtained E_g values sharply decrease with the increasing pressure. The robust band gap is still as large as 2.3 eV up to 67.4 GPa, indicating that the localized electron is so hard to transfer to the conduction band and is highly tunable. There is a method to obtain the band gap from the position of the peak energy in PL. Taking into account the binding energy of the exciton, absorption modes and the Stokes shift can be explained by the change of PL in various pressures. In addition, the previous work demonstrated the binding energy of excitons for ground states is increased with pressure.^{28,35} At 19, 30.7, and 46.8 GPa, inflection points in the sharply falling band gap were observed, which indicates structural phase transitions. Combining with the PL spectrum, the new peak at low energy is observed at ~22 GPa, and the inflection point in the redshift of intrinsic PL is also observed at similar pressure, suggesting that the decreasing band gap may be promoted by the deep Mn²⁺ centers. Above 46.8 GPa, the slow redshift and reduced intensity of PL are due to the enhanced scattering of ground state electrons by the close packing structure.

4. DISCUSSION AND CONCLUSIONS

We observed the pressure-induced two-color photoluminescence in MnCl₂ at room temperature. This kind of PL of MnCl₂ originates from two distinct Mn²⁺ emission bands in different high-pressure structural phases. MnCl₂ shows strong red luminescence, which is due to the crystal field transition $^4T_{1g}(G) \rightarrow ^6A_{1g}(S)$ of the Mn²⁺ ion at an ambient condition. The ground state of Mn has a $t_{2g}^3e_g^2$ configuration, whereas the excited state has a $t_{2g}^4e_g^1$ configuration.¹⁸ The mechanism of the de-excitation process for Mn²⁺ is shown in Figure 5. The energy levels of the free Mn²⁺ is nondegenerated in the crystal field. The energy transfer E → T governs the peaks of PL. At an ambient condition, the red PL mainly occurs through the eightfold-coordinated Mn²⁺ in the rhombohedral structure. The different emission bands correspond to the different symmetries of Mn²⁺ centers in the crystal structure. In order to further interpret the excited-state dynamics of Mn²⁺ at high pressure, we combine the UV-vis absorption spectrum, XRD, and Raman scattering to give our understanding. In the initial structure phase, the Mn and Cl form an octahedron in a CdCl₂-type structure and a little of the MnCl₂·H₂O structure. The new peak of PL is observed at 4 GPa, which means the new luminous band at 905 nm is excited. According to the

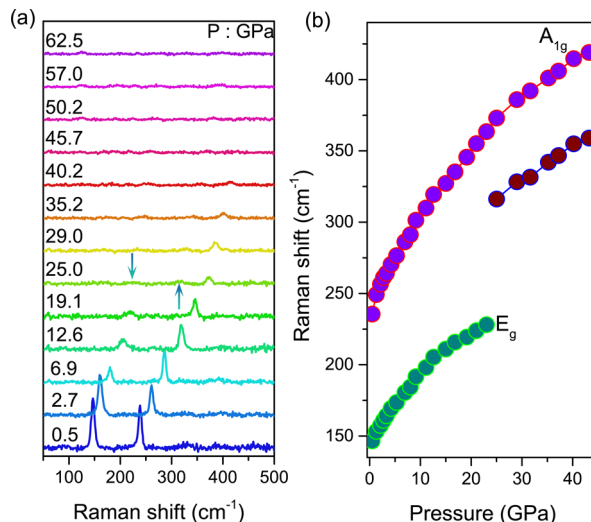


Figure 3. (a) Representative Raman spectra at various pressures for MnCl₂. (b) Pressure dependence of Raman frequency shifts.

weaker Raman peaks shift to a high frequency with the increasing pressure. With continuous compression, the E_{1g}¹ mode disappeared at 23 GPa, and the new Raman peak is observed at 25 GPa, which indicates the changes of symmetry in MnCl₂. Above 45.7 GPa, almost all of the Raman peaks disappeared, which can be explained by the structural symmetry that does not allow for Raman activity. All of the changes of the Raman peaks are in good agreement with the XRD data. All the Raman modes shifted to higher frequencies

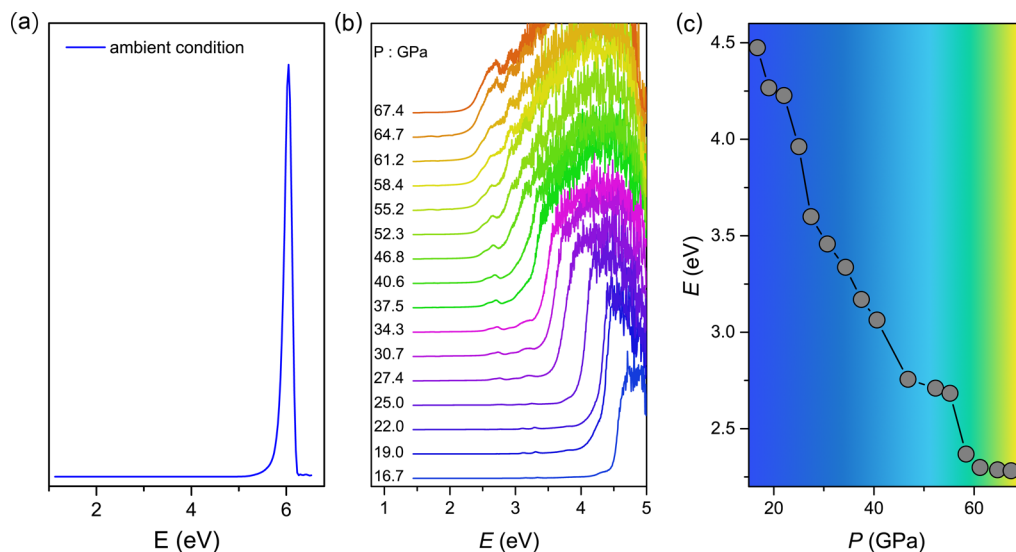


Figure 4. (a) UV–visible absorption spectrum at an ambient condition. (b) Selected optical absorption spectra of MnCl₂ at high pressures. (c) Band gap evolution of MnCl₂ at high pressure up to 67.4 GPa. The gray symbols are for compression.

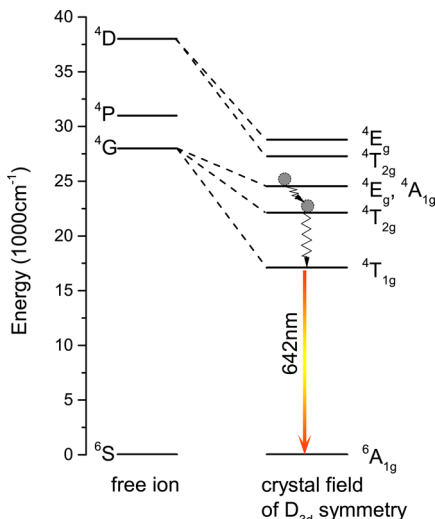


Figure 5. Energy-level diagram of Mn²⁺ in a free-ion state and in a MnCl₂ crystal.

XRD data, with the increase of pressure, the combined water disappeared due to its weak binding, and the MnCl₂ underwent the first structural phase transition that occurs at 4 GPa. The new structure was indexed by a tetragonal structure. The shrinkage of the interlayer in MnCl₂ is associated with the changes of the crystal field for Mn²⁺ centers. With continuous compression, another peak of PL was observed at 693.9 nm at 22 GPa. The second phase transition was also observed at 21.7 GPa. Thus, the mechanism of the new peak of PL can be interpreted that pressure induced a new Mn²⁺ center in the second structure phase of MnCl₂. The new Raman peak was observed at 25 GPa, which also supports the effect of the structural phase transition on Mn²⁺ centers. Up to 47.2 GPa, the third structural phase transition was observed again, and all of the Raman peaks disappeared. It is worth noting that the original emission band is quenched at 40 GPa, while the new emission band is still unquenched at 50 GPa. The pressure-induced emission band in MnCl₂ was correlated with structural phase transition. Furthermore, the PL of Mn²⁺ centers depends

on distortion and defects of the crystal lattice at a high pressure condition.

Hernandez *et al.* reported the pressure-induced two-color photoluminescence in MnF₂. The Mn²⁺ emission appears just due to phase transition. The results of the lifetime of fluorescence experiments indicate the reduction of the exchange interaction, and hence the energy transfer rate at high pressure.³⁶ It was found that interactions of the 3d electrons of Mn²⁺ is mainly affected by the crystal field interaction.³⁷ The direct excitation of the trap state is the same with the Mn²⁺ luminescence.³⁸ In addition, Falk *et al.* considered that the energy transfer from the exciton state into the Mn²⁺ shell is a dipole–dipole mechanism in the MnSe structure.³⁹ Although these previous works indicated the behavior of 3d electrons of Mn²⁺ were tuned by external conditions, the presence of PL of MnCl₂ was interpreted by the change of Mn²⁺ centers in the crystal field. Thus, our results demonstrate a clear relationship between structural phase transitions and pressure-induced two-color PL in MnCl₂.

Our main conclusions of the present work are as follows: First, the unusual red PL was observed in MnCl₂ at ambient pressure that was associated with the Mn²⁺ ions. Second, pressure-induced two-color PL are interpreted as structural phase transitions at 4 and 21.7 GPa, respectively. The luminescence of Mn²⁺ centers was affected by distortion and defects of the crystal lattice at high pressure. Third, the second and third structural phases were determined to be tetragonal structures ($P\bar{4}m2$ and $I4_1/a$). However, the fourth phase is not determined. The high-pressure structures require more efforts to be precisely determined in our future investigations. The robust new emission band of MnCl₂ is not unquenched at 50 GPa. The narrowing band gap is consistent with the structural phase transition. We discovered that the band gap rapidly decreases with increasing pressure in the third phase. The $^4T_{1g}(G) \rightarrow ^6A_{1g}(S)$ photon transitions is related with the A_{1g}^{-1} Raman mode. Our findings highlight the role of pressure in obtaining PL in concentrated materials at room temperature and provide new insights into improving photoluminescence materials.

■ ASSOCIATED CONTENT

SI Supporting Information

The Supporting Information is available free of charge at <https://pubs.acs.org/doi/10.1021/acs.jpcc.0c06598>.

Candidate structures of the fourth phase was simulated by theoretical calculation under pressure ([PDF](#))

■ AUTHOR INFORMATION

Corresponding Authors

Guoying Gao — Center for High Pressure Science (CHIPS), State Key Laboratory of Metastable Materials Science and Technology, Yanshan University, Qinhuangdao, Hebei 066004, China;  orcid.org/0000-0003-3823-2942; Email: gaoguoying@ysu.edu.cn

Lin Wang — Center for High Pressure Science (CHIPS), State Key Laboratory of Metastable Materials Science and Technology, Yanshan University, Qinhuangdao, Hebei 066004, China;  orcid.org/0000-0003-2931-7629; Phone: +86-021-80777069; Email: linwang@ysu.edu.cn

Authors

Zhipeng Yan — Center for High Pressure Science and Technology Advanced Research (HPSTAR), Shanghai 201203, China

Nana Li — Center for High Pressure Science and Technology Advanced Research (HPSTAR), Shanghai 201203, China

Linyan Wang — Center for High Pressure Science (CHIPS), State Key Laboratory of Metastable Materials Science and Technology, Yanshan University, Qinhuangdao, Hebei 066004, China

Zhenhai Yu — School of Physical Science and Technology, Shanghai Tech University, Shanghai 201210, China;  orcid.org/0000-0001-6723-116X

Mingtao Li — Center for High Pressure Science and Technology Advanced Research (HPSTAR), Shanghai 201203, China

Jinbo Zhang — College of Physical Science and Technology, Yangzhou University, Yangzhou 225002, China

Xiaodong Li — Institute of High Energy Physics Chinese Academy of Sciences, Beijing 100049, China;  orcid.org/0000-0002-2290-1198

Ke Yang — Shanghai Synchrotron Radiation Facility (SSRF), Shanghai 201800, China

Complete contact information is available at:

<https://pubs.acs.org/10.1021/acs.jpcc.0c06598>

Author Contributions

The manuscript was written through contributions of all authors. All authors have given approval to the final version of the manuscript.

Notes

The authors declare no competing financial interest.

■ ACKNOWLEDGMENTS

We acknowledge Dr. Jiaxin Zhao and Dr. Xiaolei Liu for the experimental assistance and discussion. This work is mainly supported by the Natural Science Foundation of China (grant no. 11874076), National Science Associated Funding (NSAF, grant no. U1530402), and the Science Challenging Program (grant no. TZ2016001). M.T.L. thanks the financial support from the Natural Science Foundation of China (grant no. 11804011). Portions of this work were performed at the BL15U1 beamline, Shanghai Synchrotron Radiation Facility (SSRF) in China. The authors also would like to thank the

Beijing Synchrotron Radiation Facility (BSRF) (4 W2 beamline) for the use of the synchrotron radiation facilities.

■ REFERENCES

- (1) Ajayan, P.; Kim, P.; Banerjee, K. Two-Dimensional Van Der Waals Materials. *Phys. Today* **2016**, *69*, 38–44.
- (2) Jiang, S.; Shan, J.; Mak, K. F. Electric-Field Switching of Two-Dimensional Van Der Waals Magnets. *Nat. Mater.* **2018**, *17*, 406–410.
- (3) Burch, K. S.; Mandrus, D.; Park, J.-G. Magnetism in Two-Dimensional Van Der Waals Materials. *Nature* **2018**, *563*, 47–52.
- (4) Buscema, M.; Island, J. O.; Groenendijk, D. J.; Blanter, S. I.; Steele, G. A.; van der Zant, H. S. J.; Castellanos-Gomez, A. Photocurrent Generation with Two-Dimensional Van Der Waals Semiconductors. *Chem. Soc. Rev.* **2015**, *44*, 3691–3718.
- (5) Mudd, G. W.; et al. The Direct-to-Indirect Band Gap Crossover in Two-Dimensional Van Der Waals Indium Selenide Crystals. *Sci. Rep.* **2016**, *6*, 39619.
- (6) Chubarov, V.; Suvorova, D.; Mukhieddinova, A.; Finkelshtein, A. X-Ray Fluorescence Determination of the Manganese Valence State and Speciation in Manganese Ores. *X-Ray Spectrom.* **2015**, *44*, 436–441.
- (7) Abdelaziz, M. Effect of Cs₂MnCl₂ Mixed Fillers on the Crystal Structure and Optical and Electrical Properties of Poly(Vinyl Alcohol). *J. Appl. Polym. Sci.* **2004**, *94*, 2178–2186.
- (8) Gümüs, C.; Ulutaş, C.; Ufuktepe, Y. Optical and Structural Properties of Manganese Sulfide Thin Films. *Opt. Mater.* **2007**, *29*, 1183–1187.
- (9) Liu, W.; Cera, G.; Oliveira, J. C. A.; Shen, Z.; Ackermann, L. MnCl₂-Catalyzed C–H Alkylation with Alkyl Halides. *Chem. – Eur. J.* **2017**, *23*, 11524–11528.
- (10) Heravi, M. M.; Bakhtiari, K.; Oskooie, H. A.; Taheri, S. MnCl₂-Promoted Synthesis of Quinoxaline Derivatives at Room Temperature. *Heteroat. Chem.* **2008**, *19*, 218–220.
- (11) Martínez-Martínez, R.; García, M.; Speghini, A.; Bettinelli, M.; Falcony, C.; Caldiño, U. Blue–Green–Red Luminescence from CeCl₃- and MnCl₂-Doped Hafnium Oxide Layers Prepared by Ultrasonic Spray Pyrolysis. *J. Phys.: Condens. Matter* **2008**, *20*, 395205.
- (12) Zhang, Q.; Tan, Y.; Yang, C.; Xie, H.; Han, Y. Characterization and Catalytic Application of MnCl₂ Modified Hzsm-5 Zeolites in Synthesis of Aromatics from Syngas Via Dimethyl Ether. *J. Ind. Eng. Chem.* **2013**, *19*, 975–980.
- (13) Saq'an, S. A.; Ayesh, A. S.; Zihlif, A. Optical and Thermal Properties of Poly(Ethylene Oxide) Doped with MnCl₂ Salt. *Opt. Mater.* **2004**, *24*, 629–636.
- (14) Tawansi, A.; Oraby, A. H.; Abdelrazek, E. M.; Ayad, M. I.; Abdelaziz, M. Effect of Local Structure of MnCl₂-Filled PvdF Films on Their Optical, Electrical, Electron Spin Resonance, and Magnetic Properties. *J. Appl. Polym. Sci.* **1998**, *70*, 1437–1445.
- (15) Ronda, C. R.; Siekman, H. H.; Haas, C. Photoluminescence and Absorption of MnCl₂, MnBr₂ and MnI₂. *Physica B+C* **1987**, *144*, 331–340.
- (16) Sugiura, C. X-Ray Kβ Emission and K Absorption Spectra of Chlorine in MnCl₂, FeCl₂, CoCl₂ and NiCl₂. *J. Phys. Soc. Jpn.* **1972**, *33*, 455–458.
- (17) Zidan, H. M. Electron Spin Resonance and Ultraviolet Spectral Analysis of Uv-Irradiated Pva Films Filled with MnCl₂ and Crf₃. *J. Appl. Polym. Sci.* **2003**, *88*, 104–111.
- (18) Weber, M. J. Inorganic Scintillators: Today and Tomorrow. *J. Lumin.* **2002**, *100*, 35–45.
- (19) Huang, Y.; et al. Li-Ion Battery Material under High Pressure: Amorphization and Enhanced Conductivity of Li₄Ti₅O₁₂. *Natl. Sci. Rev.* **2019**, *6*, 239–246.
- (20) Yuan, Y.; Li, Y.; Fang, G.; Liu, G.; Pei, C.; Li, X.; Zheng, H.; Yang, K.; Wang, L. Stoichiometric Evolutions of Ph₃ under High Pressure: Implication for High-T_c Superconducting Hydrides. *Natl. Sci. Rev.* **2019**, *6*, 524–531.
- (21) Zhang, L.; Liu, C.; Wang, L.; Liu, C.; Wang, K.; Zou, B. Pressure-Induced Emission Enhancement, Band-Gap Narrowing, and

Metallization of Halide Perovskite $\text{Cs}_3\text{bi}_2\text{i}_9$. *Angew. Chem., Int. Ed.* **2018**, *57*, 11213–11217.

(22) Liu, G.; Kong, L.; Yang, W.; Mao, H.-K. Pressure Engineering of Photovoltaic Perovskites. *Mater. Today* **2019**, *27*, 91–106.

(23) Mao, H. K.; Xu, J.; Bell, P. M. Calibration of the Ruby Pressure Gauge to 800 Kbar under Quasi-Hydrostatic Conditions. *J. Geophys. Res.: Solid Earth* **1986**, *91*, 4673–4676.

(24) Prescher, C.; Prakapenka, V. B. Dioptas: A Program for Reduction of Two-Dimensional X-Ray Diffraction Data and Data Exploration. *High Pressure Res.* **2015**, *35*, 223–230.

(25) Lockwood, D. J.; Christie, J. H. Electronic Raman Spectra of Co^{2+} in CdCl_2 , CdBr_2 and MnCl_2 . *Chem. Phys. Lett.* **1971**, *9*, 559–563.

(26) Lockwood, D. J. Lattice Vibrations of CdCl_2 , CdBr_2 , MnCl_2 , and CoCl_2 : Infrared and Raman Spectra*. *J. Opt. Soc. Am.* **1973**, *63*, 374–382.

(27) Wyckoff, R. W. G. Second Edition Interscience Publishers, New York, New York Fluorite Structure. *Cryst. Struct.* **1963**, *1*, 239–444.

(28) Sukumar, B.; Navaneethakrishnan, K. Effect of the Dielectric Function and Pressure on the Binding Energies of Excitons in Gaas and $\text{GaAs}/\text{Ga}_{1-x}\text{Al}_x\text{As}$ Superlattices. *Solid State Commun.* **1990**, *76*, 561–564.

(29) Ha, S. H.; Ban, S. L. Binding Energies of Excitons in a Strained Wurtzite Gan/Algan Quantum Well Influenced by Screening and Hydrostatic Pressure. *J. Phys.: Condens. Matter* **2008**, *20*, No. 085218.

(30) Zhao, G.; Liang, X. X.; Ban, S. L. Binding Energies of Excitons in Gaas/Alas Quantum Wells under Pressure. *Mod. Phys. Lett. B* **2003**, *17*, 863–870.

(31) Tornero, J. D. F. Single Crystal Structure Refinement of MnCl_2 . *Z. Kristallogr. - Cryst. Mater.* **1990**, *192*, 147.

(32) Wang, Y.; Lv, J.; Zhu, L.; Ma, Y. Crystal Structure Prediction Via Particle-Swarm Optimization. *Phys. Rev. B* **2010**, *82*, No. 094116.

(33) Wang, Y.; Lv, J.; Zhu, L.; Ma, Y. Calypso: A Method for Crystal Structure Prediction. *Comput. Phys. Commun.* **2012**, *183*, 2063–2070.

(34) Gao, B.; Gao, P.; Lu, S.; Lv, J.; Wang, Y.; Ma, Y. Interface Structure Prediction Via Calypso Method. *Sci. Bull.* **2019**, *64*, 301–309.

(35) Venkateswaran, U.; Chandrasekhar, M.; Chandrasekhar, H. R.; Vojak, B. A.; Chambers, F. A.; Meese, J. M. High-Pressure Studies of $\text{GaAs}/\text{Ga}_{1-x}\text{Al}_x\text{As}$ Quantum Wells of Widths 26 to 150 Å. *Phys. Rev. B* **1986**, *33*, 8416–8423.

(36) Hernández, I.; Rodríguez, F.; Hochheimer, H. D. Pressure-Induced Two-Color Photoluminescence in MnF_2 at Room Temperature. *Phys. Rev. Lett.* **2007**, *99*, No. 027403.

(37) Tanaka, M.; Masumoto, Y. Energy Transfer Mechanism in Mn^{2+} Doped Cds Nanocrystals. *Solid State Commun.* **2001**, *120*, 7–10.

(38) Tanaka, M. Photoluminescence Properties of Mn^{2+} -Doped II-VI Semiconductor Nanocrystals. *J. Lumin.* **2002**, *100*, 163–173.

(39) Falk, H.; Heimbrot, W.; Klar, P. J.; Hübner, J.; Oestreich, M.; Rühle, W. W. Spin-Dependent Energy Transfer from Exciton States into the $\text{Mn}^{2+}(3d^5)$ Internal Transitions. *Phys. Status Solidi B* **2002**, *229*, 781–785.